l	Supplementary file
2	Pore-scale simulation of permeability evolution induced by mineral precipitation
3	during reactive transport
4	Heng Li <sup>1, 2, 3</sup> , Fugang Wang <sup>3,*</sup> , Tianhao Wu <sup>1</sup> , Yilong Yuan <sup>3</sup> , Huixing Zhu <sup>3</sup> , Jie Liu <sup>4</sup>
5 6	<sup>1</sup> Eastern Institute for Advanced Study, Eastern Institute of Technology, Ningbo, Zhejiang 315200, P. R. China
7 8	<sup>2</sup> Department of Modern Mechanics, University of Science and Technology of China, Hefei 230027, P. R. China
9 10	<sup>3</sup> Key Laboratory of Groundwater Resources and Environment, Ministry of Education, Jilin University, Changchun 130021, P. R. China
11 12	<sup>4</sup> Physical Science and Engineering Division, King Abdullah University of Science and Technology, Thuwal 23955-6900, Saudi Arabia
13 14 15	E-mail address: hengli@eitech.edu.cn (H. Li); wangfugang@jlu.edu.cn (F. Wang); twu@eitech.edu.cn (T. Wu); yuanyl14@mails.jlu.edu.cn (Y. Yuan); zhuhx@jlu.edu.cn (H. Zhu); jie.liu.1@kaust.edu.sa (J. Liu).
16 17	*Corresponding author (ORCID: 0000-0001-5360-7808 (F. Wang))  Li, H., Wang, F., Wu, T., Yuan, Y., Zhu, H., Liu, J. Pore-scale simulation of permeability evolution
18	induced by mineral precipitation during reactive transport. Advances in Geo-Energy Research, 2025,
19 20	18(2): 109-120.  The link to this file is: https://doi.org/10.46690/ager.2025.11.02
21	The line to this inc is. https://wor.org/10.400/0/aget/2025.11.02

## Introduction

- 23 In this Supporting Information, the numerical implementation tools and relevant verifications
- of the model are introduced in detail. And the results of the power law regression analysis of
- 25 the porosity-permeability relationships are also presented here in tabular form.

26

27

28

29

30

31

32

33

34

35

36

37

38

39

40

41

42

43

44

22

## **Text S1. Numerical implementation**

The fluid flow and transport equations are solved using OpenFOAM, an open-source computational fluid dynamics (CFD) framework, which employs a finite volume discretization of space. Detailed numerical implementation of OpenFOAM can be found in previous studies (Jasak, 1996; Weller et al., 1998). The PISO algorithm, which is employed for equation solving, is elaborated in detail in a recent publication (Moukalled et al., 2016). Interface movement is handled via the Arbitrary Lagrangian-Eulerian (ALE) method, previously implemented in the dissolFoam solvers (Starchenko et al., 2016), as discussed in a recent review (Molins et al., 2021). In summary, the numerical approach integrates the pisoFoam solver for transient incompressible flows (based on the PISO algorithm), the transient convection-diffusion equations, a dynamic volumetric mesh, and the dissolFoam solver for boundary mesh adaptation, all within OpenFOAM. Topological adjustments to the initial mesh are essential, as the evolving structures can exhibit significant irregularities in shape. In the present implementation, OpenFOAM's meshing tool, snappyHexMesh, is utilized to redraw the mesh at varying intervals, determined by the instability of growth and surface roughness. Greater dendrite curvature leads to more rapid and pronounced distortion of the mesh. In all simulations, the standard interval for remeshing is set to 1000 time steps.

Furthermore, all simulations begin with the steady-state solution of flow and reactant concentration. During the simulation process, the transient Eqs. (2) and (3) are solved and coupled with dynamic grid motion until the grid becomes highly distorted and requires remeshing. At this point, the grid is redrawn, and the OpenFOAM domain mapping tool mapFieldsPar is used to transfer the field data from the old mesh to the new mesh. The mapping method option correctedCellVolumeWeight is applied to achieve weighted interpolation based on grid volume. After mapping the volume field to the new grid, the simulation (including the transient equation of the dynamic grid) is restarted. Thus, one simulation periodicity is completed. During the simulation process, when severe mesh distortion occurs, a remeshing operation is performed. This usually refers to dynamic mesh technology, which is used in OpenFOAM with the solver dynamicFvMesh. The solver monitors the mesh quality (such as maximum distortion rate, minimum volume) in real-time. When the quality of a mesh element falls below a set threshold, remeshing is triggered. The current flow field (velocity, pressure, etc.) is mapped onto the new mesh. OpenFOAM uses a conservative interpolation method to accomplish this. The specific process is as follows: (1) Particle motion causes changes in the position and shape of the geometric surface (STL or OBJ files), (2) Remeshing is triggered, (3) Call snappyHexMesh, using the same exact method but based on the updated particle surface STL (or OBJ) file, to regenerate a set of meshes that fit the new geometric shape, (4) Map the flow field and concentration field variables from the old mesh onto the new mesh, (5)

## Text S2. Relevant verification of the model

Continue calculations.

45

46

47

48

49

50

51

52

53

54

55

56

57

58

59

60

61

62

63

64

65

66

67

68

69

For the verification of the model, due to limitations such as laboratory conditions and the lack of appropriate experimental tools, relevant experiments cannot be carried out at present. For the analytical solution of the model, since the nucleation process in the article is a

probabilistic event, there is no definite analytical solution corresponding to it yet. On the other hand, in simulating the dissolution process without considering nucleation, the model (dissolFoam) used in this paper has been well verified, including comparisons with other numerical models (Fig. 1S) (Li et al., 2023). For precipitation, the Darcy-Brinkman-Stokes (DBS) model (or the OpenFOAM-DBS in Fig. S1) based on CNT has a good similarity in precipitation pattern compared with the experimental result of Yuan et al. (2021) in Fig. 2S (Yang et al., 2024). Looking forward to the future, the author will focus on strengthening the experimental verification of our model.

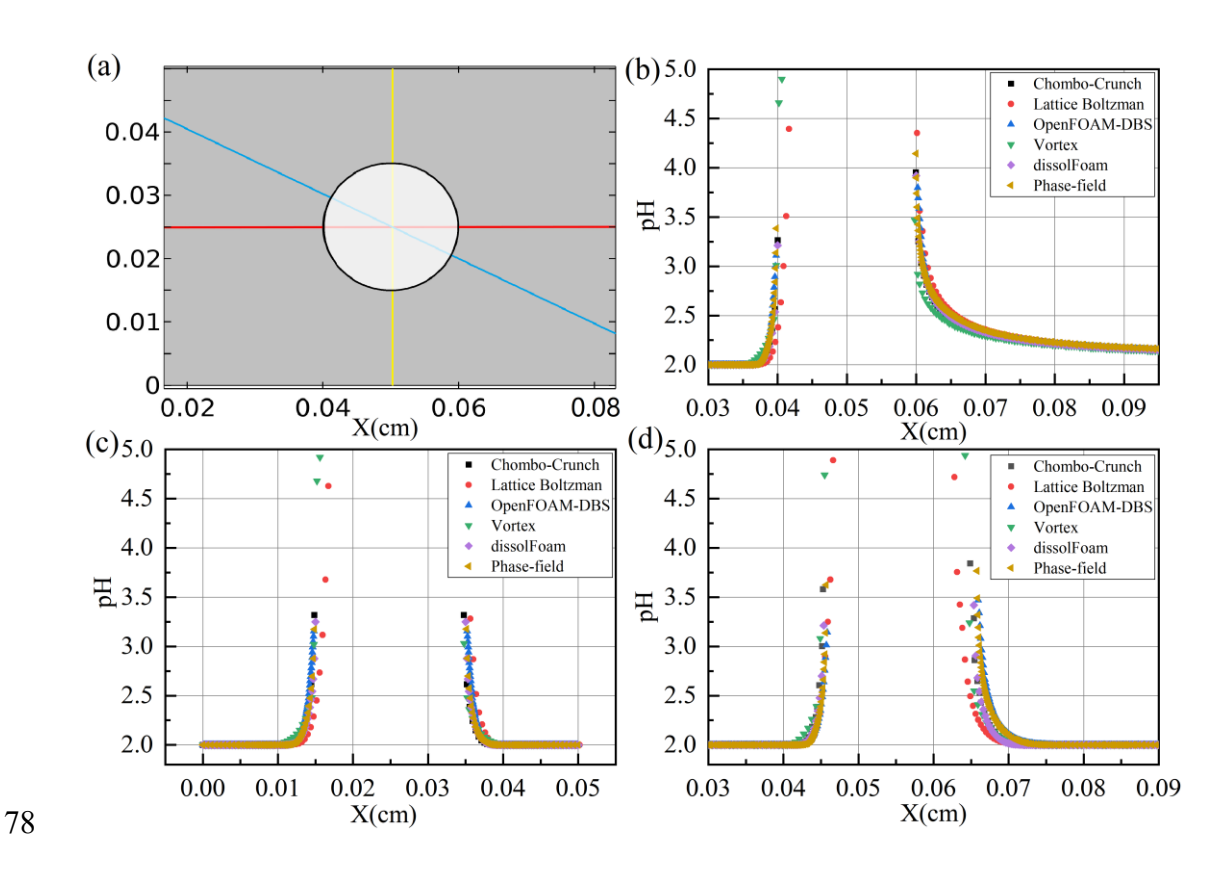


**Fig. 1S.** The pH values of the model (dissolFoam) along the horizontal transect (b), vertical transect (c), and diagonal transect (d) compared with other codes, (a) is a transversal diagram (Li et al., 2023).

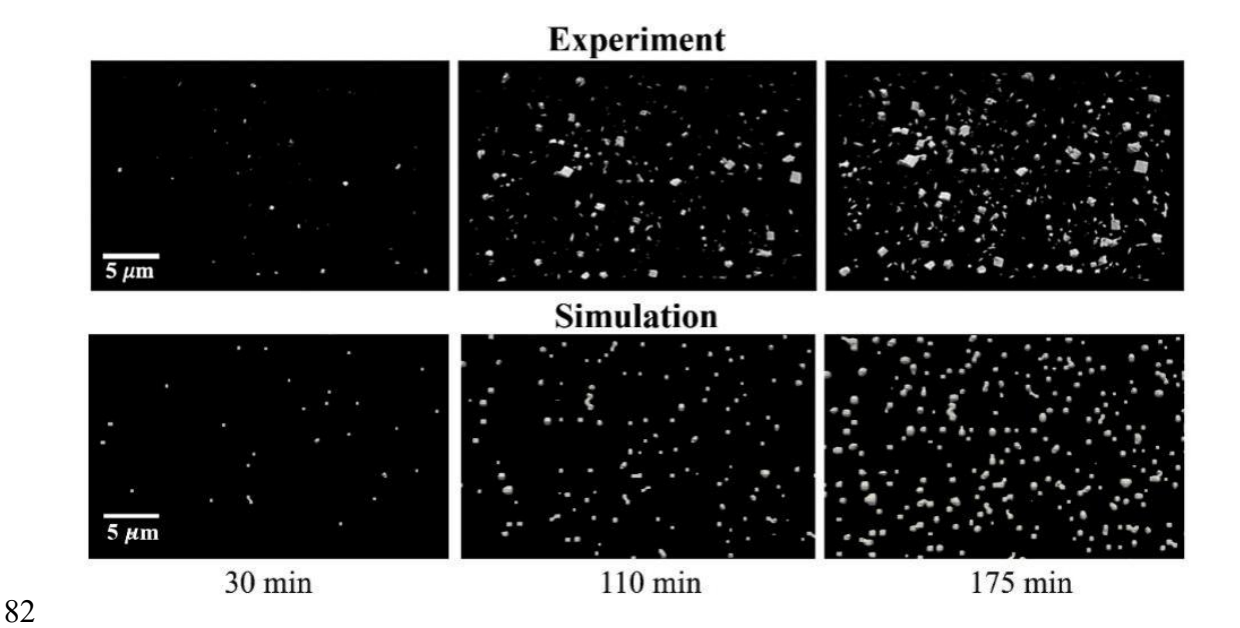


Fig. S2. The comparison of temporal evolution of nuclei on tube wall between simulation and XnT experiment for barite in SI = 2.47 solution (Yang et al., 2024).

## References

85

94

95

- Jasak, H. Error Analysis and Estimation for the Finite Volume Method With Applications to
   Fluid Flows. London, University of London, 1996.
- Li, H., Wang, F., Wang, Y., et al. Phase-field modeling of coupled reactive transport and pore structure evolution due to mineral dissolution in porous media. Journal of Hydrology, 2023, 619: 129363.
- Molins, S., Soulaine, C., Prasianakis, N. I., et al. Simulation of mineral dissolution at the pore scale with evolving fluid-solid interfaces: review of approaches and benchmark problem set. Computational Geosciences, 2021, 25(4): 1285-1318.
  - Moukalled, F., Mangani, L., Darwish, M. The Finite Volume Method in Computational Fluid Dynamics. Cham, Germany, Springer, 2016.

96	Starchenko, V., Marra, C. J., Ladd, A. J. C. Three-dimensional simulations of fracture
97	dissolution. Journal of Geophysical Research: Solid Earth, 2016, 121(9): 6421-6444.
98	Weller, H. G., Tabor, G., Jasak, H., et al. A tensorial approach to computational continuum
99	mechanics using object-oriented techniques. Computer in Physics, 1998, 12(6):
100	620-631.
101	Yang, F., Guan, D., Starchenko, V., et al. Effect of Nucleation Heterogeneity on Mineral
102	Precipitation in Confined Environments. Geophysical Research Letters, 2024, 51(9):
103	e2023GL107185.
104	Yuan, K., Starchenko, V., Rampal, N., et al. Opposing Effects of Impurity Ion Sr <sup>2+</sup> on the
105	Heterogeneous Nucleation and Growth of Barite (BaSO <sub>4</sub> ). Crystal Growth & Design,
106	2021, 21(10): 5828-5839.
107	